JOURNAL OF PHYSICAL ORGANIC CHEMISTRY
J. Phys. Org. Chem. 2003; **16:** 669–674
DOI: 10.1002/poc.649

Reaction of lithium metal with benzil in THF. A kinetic study

Norma Sbarbati Nudelman,[1]* Susana Velurtas[2] and Maria A. Grela[2]

[1]Dpto. Química Orgánica, Facultad de Ciencias Exactas, Universidad de Buenos Aires, Ciudad Universitaria, 1428 Buenos Aires, Argentina
[2]Dpto. de Química, Facultad de Ciencias Exactas, Universidad Nacional de Mar del Plata, B7602AYL Mar del Plata (BA), Argentina

Received 20 February 2003; revised 24 March 2003; accepted 26 March 2003

ABSTRACT: The kinetics of benzil reduction by lithium metal in THF were investigated under different reaction conditions. The main reaction products were phenylacetophenone and bibenzyl; 1,2-diphenylethanol and diphenylethene were minor products. The first radical anion intermediate formed by electron transfer upon chemisorption of the benzyl on the metal surface was fully characterized and quantitatively determined by ESR spectroscopy. The kinetics of the benzil decay and of the formation of the two main products were followed by GC and ESR. A unique feature of this reaction is the presence of a well-defined and reproducible induction period. A mechanism is proposed which accounts for the main experimental observations. Copyright © 2003 John Wiley & Sons, Ltd.

KEYWORDS: organolithium; benzil; lithium metal; surface reactions; induction period; heterogenous systems

INTRODUCTION

Some reactions that occur between organic compounds and specific metals have long been known, and the reaction of organic halide derivatives with magnesium, giving rise to the versatile Grignard chemistry, is one of the most useful synthetic tools available to organic chemist to assist in the assembly of complex structures in the laboratory and also useful in the preparation of many industrial chemicals.[1] Because of the continous search for new synthetic methods, other metal-mediated organic transformations are currently being studied.[2] The reducing ability of indium metal has recently been shown to have unique features because of its low first ionization potential[3,4] and its mediatory effect in powerful reactions such as the Michael reaction.[5] Reactions with other reducing metals such as zinc[6] and samarium[7] are also being developed. Mechanistic studies on these reactions are still extremely scarce; even the detailed mechanisms of the reactions of Grignard reagents have been under scrutiny by three or four generations of researchers and the work is continuing.[8] Very few kinetic studies on the reactions of metals with organic substrates have been reported. The main problem in studying heterogeneous reaction mechanisms is that of obtaining reproducible kinetic information for a clear interpretation. Thus, although experimental techniques to overcome this problem have been designed,[9,10] quantitative analysis of the mechanisms of heterogeneous reactions is sparse or almost non-existent.[11]

We have recently reported a detailed kinetic study of the reaction between benzaldehyde and lithium metal in Tetrahydrofuran (THF): the first radical intermediate was fully characterized and the reaction rates of all of the several steps involved in the overall reaction were determined.[12a] Conditions were achieved to make the reaction useful for the quantitative conversion of benzaldehyde into benzyl benzoate.[12b] This paper reports a mechanistic study of the reaction of benzil with lithium metal under well-defined reaction conditions. The reaction progress was followed both by gas chromatographic (GC) and electron spin resonance (ESR) methods, and a simplified reaction scheme is proposed to describe the main experimental observations. A brief preliminary report of this reaction was recently communicated.[13]

EXPERIMENTAL

Materials. THF was purified as described previously[14a] and was distilled from dark blue solutions of sodium benzophenone ketyl under nitrogen immediately prior to use. Benzil (Aldrich, 99%) was crystallized from ethanol, m.p. 94–95 °C (lit.[14b]). All glassware, syringes and needles were dried in a vacuum oven, cooled in a desiccator and flushed with dry nitrogen immediately prior to use.

General procedure. Lithium wire (Merck, >99%, 3 mm diameter) was weighed under ligroin, washed with THF and cut into pieces 2–3 mm long directly over a reaction

---

**Correspondence to:* N. S. Nudelman, Dpto. Química Orgánica, Facultad de Ciencias Exactas, Universidad de Buenos Aires, Ciudad Universitaria, 1428 Buenos Aires, Argentina.
E-mail: nudelman@qo.fcen.uba.ar
Contract/grant sponsor: University of Buenos Aires.
Contract/grant sponsor: University of Mar del Plata.

flask containing a small portion of boiling THF, to create a fresh surface in which the reaction could commence. The reaction flask was capped with an ‘air-tight’ stopper, and alternately evacuated and flushed with nitrogen several times, as is usually done for organolithium reactions.[15] The flask was equilibrated to the desired temperature for 15 min under vigorous magnetic stirring. A solution of benzil of the desired concentration in THF (thermostated at the same temperature) was transferred by syringe, and a 0.2 ml sample was immediately taken to verify the initial concentration, $[\mathbf{1}]_0$.

Kinetic measurements. Standard techniques for the manipulation of air- and water-sensitive compounds were strictly followed.[16] A general kinetic procedure, similar to that developed for the kinetic determinations of the reactions of naphthyllithium, was used.[17] The compositions of aliquots of the reaction mixture withdrawn at various reaction times were determined by GC and/or ESR analysis.

Rates of benzil decay and product formation, shown in Fig. 1, were measured by GC. In this case, the samples were quenched with a saturated solution of NH_4Cl and analysed using an OV-101 column (temperature gradient: 50–270 °C). In separate runs, stable products were isolated and fully characterized by mass spectrometry (using a Shimadzu QP 5050A GC–MS system), and NMR spectroscopy (determined on a Brucker 200, 300 or 500 spectrometer operating at 200, 300 or 500 MHz for ^1H and 50, 75 or 125 MHz for ^{13}C).

ESR analysis of intermediates. Well-determined volumes of the reaction mixture were placed in a quartz tube under argon and their ESR spectra were immediately recorded at 298 K using a Bruker (Germany) ER 200 X-band spectrometer. We verified that for the higher concentrations attained in our experiments the spectra of the aliquots were qualitatively invariant whereas their intensity varied slightly (<10%) over 20 min.

Radical concentrations were estimated by comparing the area under the ESR first-derivative spectrum of the sample with that of a solution of galvinoxyl, the reference standard, recorded at the same microwave power, modulation amplitude and amplification gain.

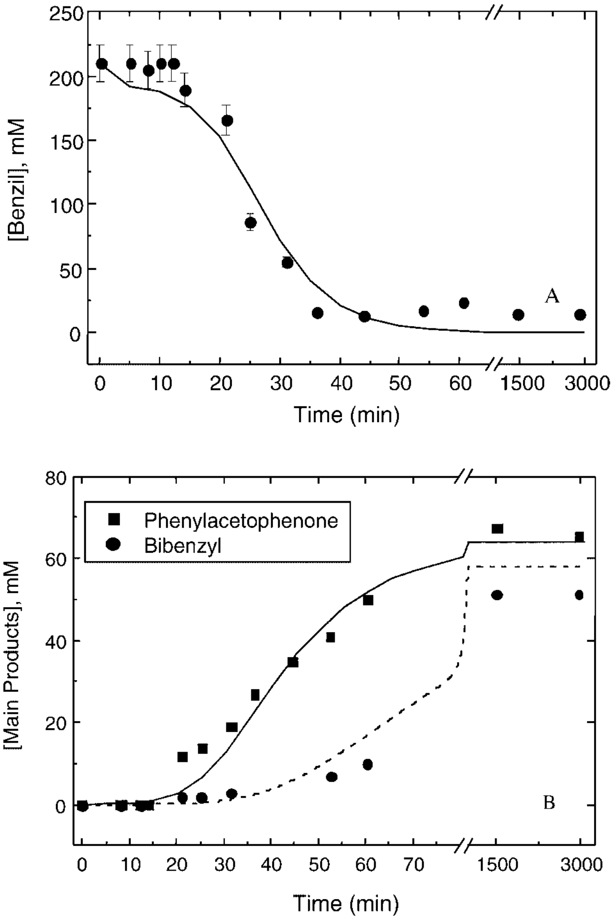

Figure 1. Reaction of lithium metal with benzil (**1**) in THF at 298 K, $[\mathbf{1}]_0 = 0.2$ M, Li = 428 mg. (A) [**1**] decay determined by GC analysis of the reaction mixture; experimental points are shown by (●); error bars are standard deviations of at least five measurements. (B) Concentration of the main reaction products, (■) [phenylacetophenone] and (●) [bibenzyl], as a function of time, determined by GC analysis. In (A) and (B), the solid lines are the simulated concentration dependence derived from the numerical integration according to the mechanism depicted in Scheme 1 and Table 1 (see the text)

RESULTS AND DISCUSSION

Reaction of benzil (**1**) with lithium metal in THF under the reaction conditions described in the Experimental section affords phenylacetophenone (**9**) and bibenzyl (**12**) as the main products, plus small amounts of 1,2-diphenylethanol (**10**) and 1,2-diphenylethene (**11**). The benzil decay and the rate of appearance of the main products were followed by GC analysis of the reaction mixture at different time intervals, as described in the Experimental section. The representative behaviour of the decay of (**1**) for the reaction in THF at 298 K is shown in Fig. 1(A) (points are experimental determinations and the bars show the dispersion range observed in at least five independent runs). As frequently found in heterogeneous reactions at liquid–solid interfaces, the reaction shows an induction time after which the reaction seems to proceed autocatalytically. It is worth remarking that the induction time was fairly reproducible. The sudden onset of benzil decay is almost coincident with the abrupt change in the solution from pale yellow to purple, the characteristic color of the benzil radical anion. Figure 1(B) shows the time-dependent appearance of the two main reaction products determined by GC. The curves also show an induction period. The lag in time for the formation of phenylacetophenone is very similar to that shown in Fig. 1(A) for the decay of **1**.

The ESR analysis of the reaction mixture at different time intervals revealed the involvement of the expected benzil radical anion as the most important radical

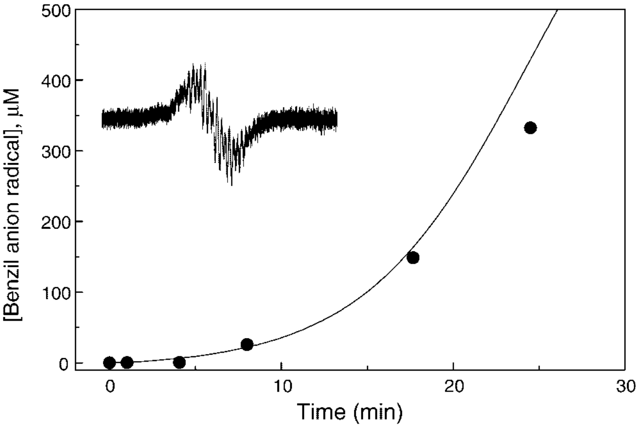

Figure 2. Reaction of lithium metal with benzil (**1**) in THF at 298 K, $[\mathbf{1}]_0 = 0.2$ M, Li = 428 mg. (●) Benzil anion radical concentration determined by ESR analysis of the reaction mixture as a function of time. Experimental conditions as in Fig. 1. The solid line is the simulated concentration dependence derived from the numerical integration according to the mechanism depicted in Scheme 1 and Table 1 (see the text)

intermediate. The ESR spectrum of the reaction mixture in THF ([**1**] = 0.2 M, Li = 428 mg) at 298 K after 20 min of reaction was reported recently.[13] The spectral total width (0.76 mT) and its hyperfine structure are fully consistent with previous reports on the benzil radical anion ([coupling constants: $a_H = 0.99$ G (4); 0.36 G (4) and 1.12 G (2) for the *ortho-*, *meta-* and *para*-H, respectively[18]]). The paramagnetic signal appears after an induction time in close correspondence with that observed for the decay of **1** by GC and it grows steadily. It is worth emphasizing that the spectral characteristics of the aliquots, taken up to 80% of benzil disappearance, remain almost the same. This fact is taken as evidence that, if not the unique, the benzil radical anion is the overwhelming radical intermediate.

Figure 2 shows the rate of formation of the benzil radical anion (**2**); the concentration of **2** was determined by ESR analysis of the reaction mixture at different time intervals. An induction period is also observed for the appearance of the radical anion. The induction time is apparently shorter than that shown in Fig. 1(A), which is consistent with the fact that the decay of **1** to give the radical anion is not detected by GC. It also indicates that further reaction of **2** to give the precursors to the first reaction product should be relatively slow.

A complete reaction mechanism able to interpret the observed results is depicted in Scheme 1. Adsorption of the reagent on the lithium surface, (symbolized by $\mathbf{1}_S$; the rate measured by k_S), is postulated to be the initial step in the reaction of **1** with Li. With the current molecular level understanding of surface reactions, it is known that adsorption plays an essential role.[10] In our previous study we also observed that adsorption of benzaldehyde on the lithium surface was very important: determination of the concentration of benzaldehyde immediately after putting the THF solution in contact with lithium showed that only 27% of the benzaldehyde remained in solution, the rest being adsorbed on the metal surface.[12] Adsorption and desorption are, then, the first phenomena which are shown in a simplified way in Scheme 1 as the two first steps. In all the reaction steps shown in Table 1, subscript **S** is used to distinguish an adsorbed from a free diffusing species in solution.

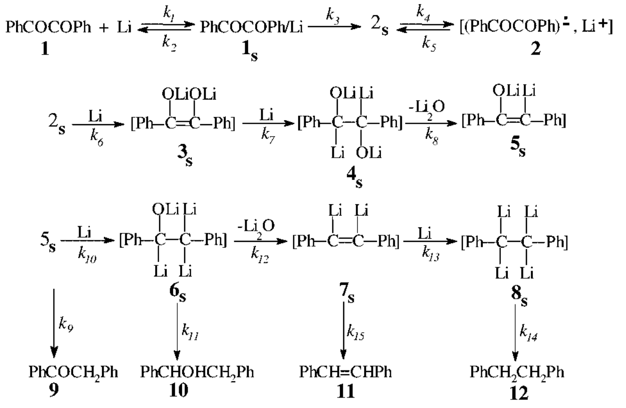

Scheme 1

It is well known that lithium has a strong tendency to lose ions into a solution.[19] Ion solvation drives this process, which is relatively easy in THF because of its known ability for cation solvation. Electron transfer from the lithium surface to the adsorbed benzil ($\mathbf{1}_S$ in Scheme 1; the rate of ET measured by k_3) produces the adsorbed [benzil radical anion–(**2**)–lithium cation] pair, symbolized by $\mathbf{2}_S$, that is also strongly solvated by THF. Species **2** partially escapes from the surface (and the solvent cage), goes into solution and can be detected by ESR in the reaction solution.

There is still controversy as to whether formation of the Grignard reagents takes place on the magnesium surface (called the A model)[20] or after the radical has diffused into solution (called the D model).[21] In the present case, sorption and desorption of the radical anion (processes 5 and 4, respectively, in Table 1) need to be considered to

Table 1. Reaction of benzil with lithium in THF at 298 K: reaction steps as in Scheme 1

No.	Reaction step	k (s^{-1})
1	$\mathbf{1} \rightarrow \mathbf{1}_s$	8.3×10^{-3}
2	$\mathbf{1}_s \rightarrow \mathbf{1}$	1.0×10^{-1}
3	$\mathbf{1}_s + S \rightarrow \mathbf{2}_s + 2\,S$	2.1×10^{-4}
4	$\mathbf{2}_s \rightarrow \mathbf{2}$	1.3×10^{-4}
5	$\mathbf{2} \rightarrow \mathbf{2}_s$	1.7×10^{-2}
6	$\mathbf{2}_s \rightarrow \mathbf{3}_s$	6.7×10^{-4}
7	$\mathbf{3}_s \rightarrow \mathbf{4}_s$	1.0×10^{-1}
8	$\mathbf{4}_s \rightarrow \mathbf{5}_s$	1.7×10^{-2}
9	$\mathbf{5}_s \rightarrow \mathbf{5}\ (\rightarrow \mathbf{9})$	2.2×10^{-2}
10	$\mathbf{5}_s \rightarrow \mathbf{6}_s$	5.0×10^{-2}
11	$\mathbf{6}_s \rightarrow \mathbf{6}_s\ (\rightarrow \mathbf{10})$	3.7×10^{-2}
12	$\mathbf{6}_s \rightarrow \mathbf{7}_s$	3.0×10^{-2}
13	$\mathbf{7}_s \rightarrow \mathbf{8}_s$	5.0×10^{-4}
14	$\mathbf{8}_s \rightarrow \mathbf{8}\ (\rightarrow \mathbf{12})$	2.5×10^{-3}
15	$\mathbf{7}_s \rightarrow \mathbf{7}\ (\rightarrow \mathbf{11})$	5.0×10^{-6}

obtain curves that fit the experimental results. As can be observed, the rate of adsorption of the radical is faster than its desorption. Most of the rest of the reactions involve reduction by lithium metal and they are assumed to occur on the surface metal in the simplified reaction scheme.

Thus, further successive reductions of **2** by the lithium metal gives intermediates **3** → **4**, that by loss of lithium oxide gives intermediate **5**, precursor of **9**, which is one of the main reaction products (24% yield in the first 60 min, final yield 35%). Further reduction of **5**, followed by a second loss of Li_2O and reduction of the double bond, afford, successively, intermediates **6**, **7** and **8**, which are the precursors of the other isolated products. The fact that only 5% of **12** is produced in the first 60 min of the reaction, together with the slower formation of bibenzyl shown in Fig. 1(B), can be considered as additional evidence that **5** is an intermediate in the formation of **12**. The solid lines in Fig. 1 were drawn following the numerical integrals derived from Scheme 1, that are gathered in Table 1. The yields of **10**, **11** and **12** after 24 h of reaction are 5, 6 and 24%, respectively. The above results were obtained at 298 K.

Kinetic analysis

The most striking kinetic feature of this reaction is the presence of a well-defined induction period. The observation of induction periods is a common situation in reactions occurring at solid–liquid interfaces, as for example the synthesis of Grignard and Reformatsky reagents on magnesium and zinc surfaces, respectively. The induction period in Grignard reagent formation is specially annoying since it is erratic, prolonged and, in some cases, apparently infinite.[21] Plausible hypotheses abound,[22] but there is no comprehensive, documented understanding of the factors that create the induction period or constitute initiation.[21]

A likely explanation is that the initiation consists of the removal of oxide layers which are generally present on untreated reactive metals and are passivating. Nevertheless, we did not observe any difference in the induction period when the lithium surface was carefully mechanically cleaned, or when the lithium pellets were very rapidly treated with dry methanol, immediately prior to the reaction. Similar results were observed in the Grignard reagent formation: sometimes reactions with ordinary magnesium ('Grignard' grade) initiated better than those of purer forms. Traces of transition metal impurities, such as iron, might be responsible.[23]

Whatever the reasons are that determine the presence of very few active sites where the reaction can initiate, when the reaction starts it seems that the area of the activated surface grows exponentially, since an autocatalytic behaviour is observed. In the case of magnesium, the observed activation by I_2 was proposed to be due to a reaction with Mg, that 'etched' it, thus cleaning the surface. Nevertheless, the 'doctrine of etching' was recently invalidated by careful experiments that demonstrate that the presence of $MgBr_2$ catalysed the reaction, irrespective of whether the Mg had been 'etched' or not.[24]

In order to rationalize the experimental results, including the autocatalytic behaviour, we set up the mechanism presented in Scheme 1 and Table 1. The autocatalytic behaviour is simulated indicating that *S*, the number of active sites, is incremented by the reaction. The group of differential equations for the full reaction mechanism was solved using a non-commercial numerical integration program, specially developed for this purpose. The calculated rate constants are listed in Table 1, and they proved to be adequate to simulate the experimental concentration profiles of benzil decay, and radical anion as well as product generation, as indicated by the solid lines in Figs 1(A) and (B) and 2. As usual, all the kinetic rates were calculated *prior* to the quenching of the reaction mixture, since protonation of the precursors is very fast. Then, the rate constants k_9, k_{11}, k_{15} and k_{14} geven in Table 1 are the calculated rate constants for the desorption of the precursors of products **9**–**12** (intermediates **5**–**8**), respectively.

Further experiments

In an effort to achieve a better understanding of the nature of the induction period, a series of experiments were carried out. The first variable studied was the benzil concentration. In agreement with the above kinetic treatment of the data, we observed that the induction period was highly dependent on [**1**]. As shown in Fig. 3, the induction period was significantly increased by reducing

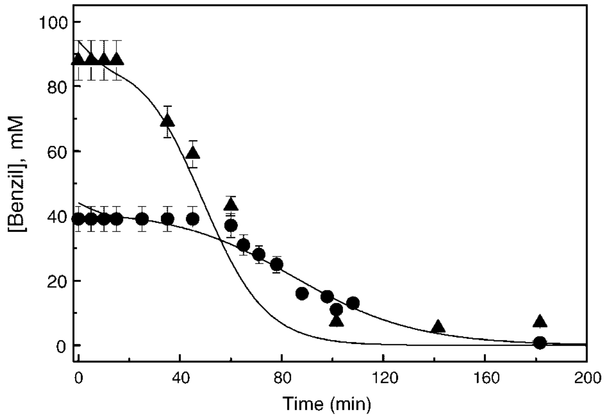

Figure 3. Reaction of lithium metal with benzil (**1**) in THF at 298 K, Li = 400 mg, at different benzil concentrations: $[\mathbf{1}]_0 = 88$ mM (▲) and 40 mM (●); benzil decay as a function of time determined by GC analysis. Solid lines are the simulated concentration dependences derived from the numerical integration, according to the mechanism depicted in Scheme 1 and Table 1 (see the text)

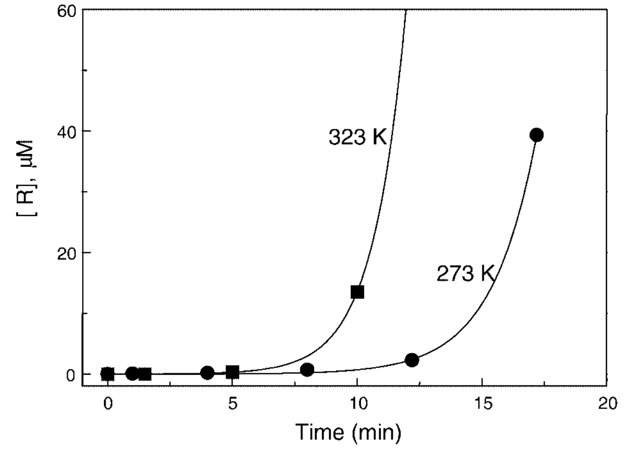

Figure 4. Reaction of lithium metal with benzil (**1**) in THF; benzil anion radical concentration versus time at 323 K (■) and 273 K (●), determined by ESR analysis of the reaction mixture. Other experimental conditions as in Fig. 1

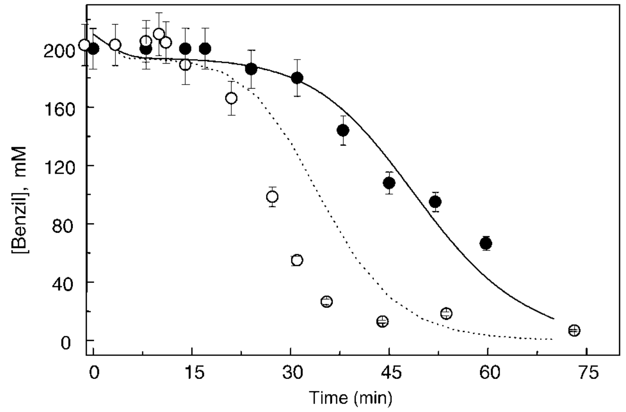

Figure 5. Reaction of lithium metal with benzil (**1**) in THF at 298 K; $[\mathbf{1}]_0 = 200$ mM. Circles are experimental data for the benzil decay under different initial lithium conditions: Li = 105 mg, 12 pellets (●); Li = 400 mg, 50 pellets (○). The broken line represents the simplified model prediction using the data in Table 1, with S proportional to the number of pellets (S is reduced from 1 to 0.24). The solid line is a simulation using $S = 0.24$ and a slightly lower value of $k_3 = 1.5 \times 10^{-4}\,\mathrm{s}^{-1}$; the rest of rate constants are as in Table 1

the benzil concentration. Note that the simplified mechanism is able to reproduce the experimental findings, as indicated by the solid lines.

The temperature effects on the reaction rates (between 273 and 323 K) were then analysed by ESR (see Fig. 4). Interestingly, we observed that the rate of radical formation, and also the induction time at 323 K, were nearly identical with those found at 298 K. However, at 273 K the onset of radical production was delayed by a few minutes (see Fig. 4). It is worth noting that this finding may simply reflect the fact that the radical anion species spends more time on the surface. In fact, we were able to detect by GC analysis of the species adsorbed at the metal surface that the degree of adsorption of benzil is considerably enhanced by reducing the temperature from 298 to 273 K.

As a further test, we analysed the influence of the total mass and the number of lithium pellets on the kinetic behaviour. If the rate of the reaction were proportional to the area, a, on lithium, then increasing a would increase the rate of reduction of **1** and of subsequent reactions and, eventually, affect the product distribution. However, it can be seen in Fig. 5 that the main difference observed for an increase in a is a change in the induction period. This finding, which may seem apparently contradictory, clearly suggests that it is the *surface modification induced by the reaction* that is rate determining and not the availability of initiation sites. This surface modification could be a sort of 'metallic corrosion;' if so, then the local-cell hypotheses could apply: Li^+ ions enter the solution and electrons leave the metal, being transferred to the adsorbed reductant. This is consistent with the fact that the reaction requires a somewhat dipolar solvent to occur; no reaction is observed in hexane or even in diethyl ether. Our results are in line with the previous 'metallic corrosion'-like hypothesis to explain the autocatalytic behaviour in Grignard reactions.[25] Another hypothesis invokes corrosion in Grignard reactions by direct chemical action.[20a] Nevertheless, there seems to be no evidence that distinguishes local-cell corrosion from direct chemical action.[21]

Several ways to increase the initial rate of a Grignard reaction have been proposed. A recent report described the activation of the Mg metal surface that allowed the initiation of the Grignard reagent formation at or below 20 °C, which is very convenient for a safe preparation on a plant scale.[26] Previous studies of the effect of ultrasound on the preparation of the magnesium had shown that presonication (in the absence of the reaction partner) had no effect on the induction time,[27] but more recent work indicated that sonication promotes initiation but does not always influence yields.[28] Scanning electron microscopy studies confirmed that the number of initiation pits is effectively increased by ultrasound.[26]

In the present case, activation of the lithium surface by using a lithium emulsion was attempted but no changes in rate or in the product distribution were observed, which is consistent with the conclusion that the only remaining explanation for the induction period and the autocatalytic behaviour is surface activation induced by the reaction.

As discussed before, in spite of the heterogenous system and a complex overall reaction scheme, the simplified mechanism in Scheme 1 and Table 1 is able to reproduce qualitatively the experimental results. Although in complex reactions, especially when dealing with heterogenous reactions, it is difficult to interpret every rate constant, some attempts can be made to check whether the calculated rate constants are in agreement with the general knowledge about the expected relative rates of each step. Thus, it is known that adsorption of neutral species on the surface is more difficult than that of charged species, whereas the opposite applies with desorption:[10] the values of the pairs of steps 1–2 and 4–5 are consistent with this. Electron transfer (ET) to carbonyl compounds has been found to be the determining step in several reactions:[17] step 3 implies an ET and is one of the slowest steps in the scheme. On the other hand, loss of lithium oxide is relatively easy in these oxyanions and has similar rates in related species (see steps 8 and 12). Steps 7 and 10 are relatively fast: this is consistent with the expectation that unsaturated oxyanions would be more easily reduced than carbonyl compounds.

A last refinement of the data treatment, trying to interpret the role of active sites, is shown in Fig. 5. The broken line represents model predictions considering S proportional to the number of pellets, and it can be observed that it is in good qualitative agreement with the experimental findings. Considering S proportional to the number of pellets, it is reduced from 1 to 0.24. A simulation using $S = 0.24$ and a slightly lower value of k_3 (the rest of the rate constants as in Table 1) gives the solid line that accounts for the reduction in rate when the number of active sites is reduced. More quantitative predictions would require the precise knowledge of S, a somewhat elusive quantity.

Although it is recognized that our experimental approach does not allow one to disentangle fully the real genesis of the autocatalytic step in this complex system, it becomes apparent that the rate of activation of the metal surface may become critically controlled by the reaction. Further work on this issue is under way.

CONCLUSIONS

This paper represents the first report of a kinetic study of the reaction of lithium metal with benzil in THF under several reaction conditions. The rates of substrate decay and those of formation of the two main reduction products (phenylacetophenone and bibenzyl) were interpreted within a reaction scheme proposed to account for the observed results. Adsorption and desorption phenomena on the lithium surface seem to play an essential role in the overall mechanism of the reaction. Formation of the first radical anion intermediate was followed by ESR and is consistent with the proposed reaction scheme. A unique feature of this reaction is the presence of a well-defined induction period, after which the reaction proceeds autocatalytically. Although the real genesis of the induction period and the autocatalysis is generally difficult to interpret, and is probably due to more than one reason, the results indicate that in the present case surface modification induced by the reaction is involved.

Acknowledgements

Financial support from the University of Buenos Aires and from the University of Mar del Plata is gratefully acknowledged.

REFERENCES

1. Busch FR, de Antonis DM. In *Grignard Reagents. New Developments*, Richey HG, Jr (ed). Wiley: Chichester, 2000; 164–183.
2. Li C-J, Chan T-H. *Organic Reactions in Aqueous Media*. Wiley: New York, 1997.
3. Hashmi ASK. *J. Prakt. Chem.* 1998; **340**: 84–88.
4. Chae H, Cho S, Keum G, Kan SB, Pae AN, Kim Y. *Tetrahedron Lett.*, 2000; **41**: 3899–3900.
5. Kan S, Jang T-S, Keum G, Kan SB, Chung BY, Han S-Y, Kim Y. *Org. Lett.*, 2000; **2**: 3615–3617.
6. Tsukinoki T, Tsuzuki H. *Green Chem.* 2001; **3**: 37–38.
7. Wan L, Zhou L, Zhang Y. *Synlett* 1999; 1065–1066.
8. Holm T, Crossland I. In *Grignard Reagents. New Developments*, Richey HG, Jr (ed). Wiley: Chichester, 2000; 1–26.
9. (a) Garst JF, Swift BL, Smith DW. *J. Am. Chem. Soc.* 1989; **111**: 234–240; (b) Garst JF, Swift BL. *J. Am. Chem. Soc.* 1989; **111**: 241–244; (c) Rogers HR, Hill CL, Fujiwara Y, Rogers RJ, Mitchell HL, Whitesides GM. *J. Am. Chem. Soc.* 1980; **102**: 217.
10. Somorjai AG. *Introduction to Surface Chemistry and Catalysis*. Wiley: New York, 1994.
11. Garst JF, Ungváry F, Baxter JT. *J. Am. Chem. Soc.* 1997; **119**: 253.
12. (a) Nudelman NS, Mendiara SN. *J. Phys. Org. Chem.* 1997; **10**: 233–237; (b) Nudelman NS, Mendiara SN. *Tetrahedron Lett.*, 1997; **38**: 2245–2248.
13. Nudelman NS, Garcia GV, Velurtas S. *J. Phys. Org. Chem.* 2002; **15**: 903–910.
14. (a) Pérez DG, Nudelman NS. *J. Org. Chem.* 1988; **53**: 408–414; (b) Vitale AA, Doctorovich FD, Nudelman NS. *J. Organom. Chem.* 1987; **332**: 9–18.
15. Nudelman NS, Garcia GV. *J. Org. Chem.* 2001; **66**: 1387–1392.
16. Shriver DF. *The Manipulation of Air Sensitive Compounds*. Wiley: New York, 1989.
17. (a) Nudelman NS, Doctorovich F. *J. Chem. Soc., Perkin Trans 2* 1994; 1233–1236; (b) Nudelman NS, Doctorovich F. *Tetrahedron* 1994; **50**: 4651–4666.
18. Maruyama K, Katagiri T. *J. Phys. Org. Chem.* 1989; **2**: 205.
19. (a) Eberson L. *Electron Transfer Reactions in Organic Chemistry*. Springer: Berlin, 1987; (b) Fox MA, Chanon M (eds). *Photoinduced Electron Transfer*. Elsevier: Amsterdam, 1988.
20. (a) Hamdouchi C, Walborsky HM. In *Handbook of Grignard Reagents*, Heinemann H (ed). Marcel Dekker: New York, 1996; 145–218; (b) Walborsky HM. *Acc. Chem. Res.* 1990; **23**: 255–256; (c) Walborsky HM, Hamdouchi C. *J. Am. Chem. Soc.* 1993; **115**: 6406–6408.
21. Garst JF, Ungvary F. In *Grignard Reagents: New Developments*, Richey HG (ed). Wiley: Chichester, 2000; 185–275.
22. Silberman GS, Rakita PE. In *Handbook of Grignard Reagents*, Heinemann H (ed). Marcel Dekker: New York, 1996.
23. Kharasch MS, Reinmuth O. *Grignard Reactions of Nonmetallic Substances*. Prentice-Hall: Englewood Cliffs, NJ, 1954.
24. Garst JF, Lawrence KE, Batlaw R, Boone JR, Ungvary F. *Inorg. Chim. Acta* 1994; **222**: 365–375.
25. (a) Markies PR, Akkerman OS, Bieckelhaupt FW, Smeets JJ, Spek AL. *J. Am. Chem. Soc.* 1988; **110**: 4284–4292; (b) De Boer HJR, Akkerman OS, Bieckelhaupt FW. *Angew. Chem.* 1988; **100**: 735–737.
26. Tilstam U, Weinmann H. *Org. Proc. Res. Dev.* 2002; **6**: 906–910.
27. Pugin B, Turner AT. Influence of Ultrasound on Reactions with Metals. In *Advances in Sonochemistry*, vol. 1. JAI Press: London; 81–118.
28. Tuulmets A, Kaubi K, Heinoja K. *Ultrasonics Sonochem.* 1995; **2**: S75–S78.